



HAL
open science

The relative contributions of various viewpoint oscillation frequencies to the perception of distance traveled

Martin Bossard, Daniel Mestre

► **To cite this version:**

Martin Bossard, Daniel Mestre. The relative contributions of various viewpoint oscillation frequencies to the perception of distance traveled. *Journal of Vision*, 2018, 18 (2), pp.3-3. 10.1167/18.2.3 . hal-01707821

HAL Id: hal-01707821

<https://hal.science/hal-01707821>

Submitted on 20 Feb 2018

HAL is a multi-disciplinary open access archive for the deposit and dissemination of scientific research documents, whether they are published or not. The documents may come from teaching and research institutions in France or abroad, or from public or private research centers.

L'archive ouverte pluridisciplinaire **HAL**, est destinée au dépôt et à la diffusion de documents scientifiques de niveau recherche, publiés ou non, émanant des établissements d'enseignement et de recherche français ou étrangers, des laboratoires publics ou privés.

The relative contributions of various viewpoint oscillation frequencies to the perception of distance traveled

Martin Bossard

Aix-Marseille Univ, CNRS, ISM, Marseille, France



Daniel R. Mestre

Aix-Marseille Univ, CNRS, ISM, Marseille, France



Humans and most animals are able to navigate in their environment, which generates sensorial information of various kinds, such as proprioceptive cues and optic flow. Previous research focusing on the visual effects of walking (bob, sway, and lunge head motion) has shown that the perception of forward self-motion experienced by static observers can be modulated by adding simulated viewpoint oscillations to the radial flow. In three experimental studies, we examined the effects of several viewpoint oscillation frequencies on static observers' perception of the distance traveled, assuming the assessment of distance traveled to be part of the path integration process. Experiment 1 showed that observers' estimates depended on the frequency of the viewpoint oscillations. In Experiment 2, increasing the viewpoint oscillation frequency actually led to an increase in the global retinal flow. It also emerged that simulated viewpoint oscillations enhance the sensation of self-motion: In a specific low-frequency range (<4 Hz), they improved subjects' estimates of the distances traveled. Lastly, in Experiment 3, observers were presented with two different simulated viewpoint oscillation patterns, both involving the same amount of global retinal motion, but in one case, the pattern simulated the visual effects of natural walking, and in the other case, the pattern was not biologically realistic. Contrary to the predictions of a previous ecological hypothesis, the subjects gave similar responses under both conditions. The global retinal motion may be mainly responsible for these effects, which were found to be optimal in a specific fairly low-oscillation frequency range.

motion to keep track of one's own position relative to the starting point (Chrastil & Warren, 2012). Classically, two main types of sensory information have been identified in the context of path integration: internal self-motion cues (idiothetic information), including efferent motor commands, reafferent proprioceptive, and vestibular information (Harris et al., 2002; Harris, Jenkin, & Zikovitz, 2000; Israël & Berthoz, 1989; Mittelstaedt & Mittelstaedt, 2001), and external environmental cues (allothetic information) coming from the spatial consequences of self-motion, such as the optic flow (Gibson, 1950), auditory flow, and haptic flow.

Because the vestibular and proprioceptive inputs involved in the path integration process (Mittelstaedt & Mittelstaedt, 1980) are known to provide subjects with information about their own movements (Harris et al., 2000; Kearns, Warren, Duchon, & Tarr, 2002), odometry (Durgin, Akagi, Gallistel, & Haiken, 2009), and especially the distance traveled in space (Campos, Butler, & Bühlhoff, 2012, 2014), it was proposed to focus here on the contribution of the optic flow and its spatiotemporal properties to subjects' self-motion perception.

With a view to understanding the sources of information involved in navigation, the authors of previous studies have created paradigms aiming at dissociating between external and internal information, particularly optic flow from other perceptual cues. When exposed to optic flow patterns (i.e., patterns simulating forward motion in depth), observers can report an illusory sensation of self-motion known as "vection." Vection can occur in real life, when passengers sitting in a stationary train experience an illusion of movement when a nearby train starts to move (Ash & Palmisano, 2012; Dichgans & Brandt, 1978; Durgin, 2009; Palmisano, Gillam, & Blackburn, 2000). This phenomenon shows that the optic flow alone can suffice to inform us about our movements in space. This is also supported by neurophysiological evidence showing that the activity of the visual cortical

Introduction

When exploring their environment, humans and other animals use a navigation strategy called path integration to estimate the distance they have traveled. Path integration is the ability to integrate multiple sources of perceptual information generated by self-

Citation: Bossard, M., & Mestre, D. R. (2018). The relative contributions of various viewpoint oscillation frequencies to the perception of distance traveled. *Journal of Vision*, 18(2):3, 1–18, <https://doi.org/10.1167/18.2.3>.

<https://doi.org/10.1167/18.2.3>

Received July 12, 2017; published February 1, 2018

ISSN 1534-7362 Copyright 2018 The Authors



This work is licensed under a Creative Commons Attribution-NonCommercial-NoDerivatives 4.0 International License.

Downloaded From: <http://jov.arvojournals.org/pdfaccess.ashx?url=/data/journals/jov/936743/> on 02/01/2018

regions increases during purely visually simulated self-motion (Brandt, Bartenstein, Janeck, & Dietrich, 1998). Gibson (1950) first established that the optic flow delivers information about the spatiotemporal relationships between an observer and his or her environment. It has meanwhile been established in several studies that both animals and humans are able to discriminate and reproduce the distance they have flown/traveled on the basis of visual cues (Bremmer & Lappe, 1999; Esch & Burns, 1996; Lappe, Bremmer, & van den Berg, 1999; Srinivasan, Zhang, Altwein, & Tautz, 2000).

The paradigms used in these studies often consisted in presenting stationary observers with a linear optic flow simulating forward self-motion in depth and asking them to carry out various distance estimation tasks (Harris et al., 2012; Redlick, Jenkin, & Harris, 2001). However, besides the linear optic flow associated with purely translational motion, it is well known that natural walking creates oscillations of the head (bob, sway, and lunge head motion) as well as three-dimensional (3D) head rotations. These visual oscillations are therefore naturally linked to the proprioceptive and vestibular information generated when we are walking, and they may therefore contribute importantly to the perception of our own movements. The authors of a few studies (Durgin, Gigone, & Scott, 2005; Kim, Chung, Nakamura, Palmisano, & Khuu, 2015; Kim & Khuu, 2014; Kim & Palmisano, 2008; Kim, Palmisano, & Bonato, 2012; Palmisano, Allison, Ash, Nakamura, & Apthorp, 2014; Palmisano et al., 2000) have examined how the visual effects of the head motion that occurs during walking contribute to self-motion perception. Kim and his colleagues have shown that adding simulated head oscillations to a radial optic flow can increase the strength of the in-depth illusion of self-motion (i.e., linear vection), but the process underlying this enhancement still remains to be explained. In many of their studies, Kim and Palmisano (2008, 2010b) attributed this enhanced visual perception of self-motion at least partly to the fact that in stationary observers, viewpoint oscillations generate similar compensatory eye movements to those that normally occur during natural walking (which stabilize the retinal image of the environment) and stimulate the parietoinsular vestibular cortex, which plays a major role in vestibular sensory integration processes (Grüsser, Pause, & Schreier, 1990).

In a previous study (Bossard, Goulon, & Mestre, 2016), we found that, compared with a purely translational optic flow, adding viewpoint oscillations (simulating the head oscillations that occur during natural walking) or rhythmical viewpoint oscillations (vertical triangular oscillations) with the same vertical frequency (2 Hz, corresponding to the step frequency of subjects walking at their preferred speed) improved the

subjects' estimation of the distance traveled. The latter results were supported by the leaky path integration model (Lappe, Jenkin, & Harris, 2007) assuming that the state variable is the current distance to the target, which has to be gradually canceled by moving toward this target. This model involves two main parameters: the sensory gain (k) corresponding to a proportionality constant, which causes the state variable to increase or decrease (depending on the sign of k) proportionally to the step length at every step, and the leak rate (α) occurring at every step, which is proportional to the current value of the state variable. In other words, the gain factor (k) describes whether the increase in each step in the integration process is larger ($k > 1$) or smaller ($k < 1$) than the actual step size.

These results may be attributable to the fact that the process of optic flow integration is subject to less leakage than in viewpoint oscillation conditions, which is partly consistent with other data on vection: When observers are presented with a simulation of linear self-motion in depth at constant speed, their perception of speed decreases over time as they adapt to the local 1D motion (Denton, 1980; Schmidt & Tiffin, 1969). Several authors have subsequently suggested that adding oscillations might maintain the subjects' sensitivity to the optic flow by reducing the subjects' motion adaptation to the translational (radial) component of the optic flow and thus improve their perception of self-motion perception (Kim & Khuu, 2014; Palmisano et al., 2014; Seno, Palmisano, & Ito, 2011). However, although Seno et al. (2011) have reported that radial flow displays including simulated vertical viewpoint jitter/oscillation induced significantly longer vection durations and significantly shorter motion after-effects than nonoscillating control displays, the subjects' adaptation to randomly jittering displays resulted in substantially longer vection after-effects than adaptation to either the oscillating or purely radial displays. Contrary to these findings, Palmisano, Kim, and Freeman (2012) reported that simulated horizontal viewpoint oscillations (with a frequency of 0.58, 0.75, or 1 Hz) significantly reduced the vection onset delays and increased the vection durations but did not significantly affect the subsequent motion after-effects in comparison with those observed under nonoscillatory conditions.

In line with our previous study (Bossard et al., 2016), in which we questioned the effects of the biological versus nonbiological (*triangular*) nature of viewpoint oscillations on self-motion perception, it was proposed here first to test the effects of various viewpoint oscillation frequencies on subjects' perception of the distance traveled. Stationary observers were therefore presented with visually-induced virtual displacements of four kinds triggered by a global optic flow presented in an immersive environment, the Cave Automatic

Virtual Environment (CAVE; Cruz-Neira, Sandin, & DeFanti, 1993). The first type of flow (called the *linear* flow) was generated by programming a “pure” translation of the virtual environment inducing a subjective illusion of forward movement at a constant speed ($1.47 \text{ m}\cdot\text{s}^{-1}$). In situations of this kind, subjects’ subjective assessment of the distance traveled is usually overestimated (i.e., they undershoot the target; Frenz & Lappe, 2005; Lappe et al., 2007; Redlick et al., 2001). The other three kinds of flows were vertical triangular oscillations with three different spatiotemporal frequencies (*low* [1 Hz], *medium* [2 Hz], and *high frequency* [4 Hz]) added to the linear forward motion at the same forward speed as in the *linear* flow. The *Medium Frequency* condition (2 Hz) presents the closest properties to visual consequences of natural walking in terms of frequency (assimilated to step frequency; $2 \text{ step}\cdot\text{s}^{-1}$) and spatial period (wavelength, assimilated to step length; 0.735 m). These parameters were based on head movements recorded during an actual walking task performed by one of the subjects in the study by Bossard et al. in 2016 (Experiment 2, Phase 1). Accordingly, to maintain the same forward speed, the spatial period of oscillations was modulated in line with the following equation: *forward speed* = *frequency* × *spatial period*. In other words, when the frequency is multiplied by two, the spatial period will be divided by two and vice versa.

These last years, authors have proposed and tested several hypotheses concerning viewpoint oscillation/jitter effects on visual self-motion perception (see Palmisano, Allison, Kim, & Bonato, 2011, for a review). In this study, we focused on four of these hypotheses, and according to them, the viewpoint oscillation frequency:

1. may modulate path integration processes, assuming viewpoint oscillations to be visual effects of the step length and the step frequency during walking, in line with the leaky path integrator model (Lappe et al., 2007);
2. may increase the global retinal motion and thus improve the sensation of self-motion (Kim & Palmisano, 2010a; Palmisano et al., 2012; Palmisano & Kim, 2009);
3. may generate pursuit eye movements, which would indirectly stimulate stationary subjects’ vestibular cortex (Kim & Palmisano, 2008)—this in turn might increase the sensation of self-motion induced; and
4. may increase the sensation of self-motion, especially at frequencies resembling the natural step frequency because of its more ecological/naturalistic nature.

In this study, it was proposed to test these four hypotheses. The first experiment was designed to test whether various viewpoint oscillation frequencies

affected the path integration, self-motion perception, and hence the distance traveled perception processes (Hypothesis 1). In the second experiment, we tested whether these same four viewpoint oscillation conditions triggered different pursuit eye and/or head movements. We then repeated Experiment 1, while measuring the subjects’ eye movements with an electro-oculographic system (EOG) and their head movements, using the CAVE motion tracking system. The aim of this experiment was to determine whether these four optic flow conditions induced different global retinal motions (Hypothesis 2) or whether the viewpoint oscillations generated compensatory pursuit eye and head movements (Hypothesis 3). The third experiment was intended to test whether or not two viewpoint oscillation conditions generating the same amount of global retinal motion but having similar or incompatible characteristics from the visual consequences of walking affect self-motion perception in the same way (Hypothesis 4).

Experiment 1

Method

Participants

Twenty volunteers (10 men and 10 women, mean age 23.15 ± 3.3 years, mean height 174.7 ± 11 cm) took part in the experiment. They had no vestibular antecedents or disorders liable to affect their locomotor performances. They all had normal or corrected-to-normal vision. All the participants gave their written informed consent prior to the experiment, in keeping with the 1964 Helsinki Declaration, and the study was approved by the local ethics committee.

Apparatus

This experiment was conducted in a large-screen immersive display (CAVE) housed in the Mediterranean Virtual Reality Center (CRVM; <http://crvm.ism.univ-amu.fr>). The CAVE setup consists of a 3-m-deep, 3-m-wide, 4-m-high cubic space surrounded by three vertical screens (the walls) and a horizontal screen (the floor). The three vertical surfaces receive back-projected images, and the ground receives direct projections with a spatial resolution of 1.400×1.050 pixels and a temporal resolution of 60 Hz.

Each projection surface was illuminated by two video projectors generating passive stereoscopic images. Stereo separation was ensured by colorimetric filters equipping each pair of projectors. The same color filters were installed on the 3D glasses worn by the subjects.



Figure 1. The experimental setup. The large screen immersive display (CAVE) at Aix-Marseille University. The participant was standing inside the CAVE facing the front wall and the infinite tunnel.

The Infitec system ensured perfect separation between the images received by each eye.

The system was able to measure the subjects' movements, thus allowing interactive exchanges with the virtual environment in real time. This interactivity was based on a tracking system (ART) involving a set of eight cameras positioned inside the CAVE. This device can be used to track the position of the observer's head in the environment, making coherent perception of the virtual environment possible.

The entire system was managed by a computer system based on a cluster of 10 PC machines equipped with professional graphic cards. This system is capable of generating synchronously and spatially realistic stereoscopic models of virtual environments coupled, in real time, with the observer's position. The ICE software, a proprietary software belonging to the Institute of Movement Science, was used to prepare and control the environmental setup and the experimental procedure, as well as dealing with individual data recordings.

The subject was standing in an "infinite" straight tunnel (Figure 1). This virtual tunnel had the same width as the CAVE (3 m) and was consistent in size with the physical scale of the CAVE. The subject was standing 1.5 m from the side screens and 3 m from the front screen of the CAVE. The tunnel floor was graphically homogeneous and therefore devoid of landmarks. Likewise, no visual indices could be used in the tunnel because of its nonsingular random texture. On the floor, the subject could see a target consisting of a "road marking" cone of the usual size (height: 70 cm).

This target was placed at an initial virtual distance of 6, 12, 18, 24, or 30 m relative to the observer, depending on the trial (Bossard et al., 2016; Plumert, Kearney, Cremer, & Recker, 2005).

Procedure

The participants, facing the front wall and therefore looking at the tunnel, and holding a two-button mouse, were given the following instructions: (1) they had to estimate the distance to a cone (the target); (2) they would first hear a beep requesting them to look straight ahead, followed by a second beep, 1 second later; and (3) after the second beep, they could trigger the onset of the trial by pressing the left button on the mouse (pressing the button had two simultaneous effects: the disappearance of the target and the virtual motion of the tunnel relative to the participant); (4) they had to click again on the button when they thought they had reached the position of the previously seen target; and (5) they were told that this task would be repeated during several trials.

While undergoing optic flow stimulation, the participants therefore had to indicate when they thought they had reached the previously memorized position of the cone (the target). When they felt they had reached the previous position of the target, they had to click again on the left button of the mouse. The second click was recorded and taken to reflect the distance virtually traveled to reach the cone. The second click also had the effect of stopping the motion of the tunnel, and after a period of 2 s had elapsed, initiated the onset of the following trial. This procedure was repeated identically in all the trials, with various initial target distances and simulation modes.

Modes of the virtual self-movement simulations: The optic flow conditions

Linear (L): In the *Linear* mode, the camera simulating the subject's viewpoint performed a strictly linear translation at the same mean velocity as in the other conditions ($1.47 \text{ m}\cdot\text{s}^{-1}$) as if the camera were moving on straight horizontal rails, aligned with the tunnel.

Medium Frequency (MF): In the *MF* condition (Figure 2), the optic flow simulated a linear translation, on which vertical triangular oscillations with an amplitude of 0.044 m were superimposed. The simulated forward speed was the same as in the *linear* condition ($1.47 \text{ m}\cdot\text{s}^{-1}$), the frequency was 2 Hz, and the spatial period was 0.735 m. These parameters were based on head movements recorded during an actual walking task performed by one of the subjects in the study by Bossard et al. (2016; Experiment 2, Phase 1). These oscillations differed from the natural human pattern in their

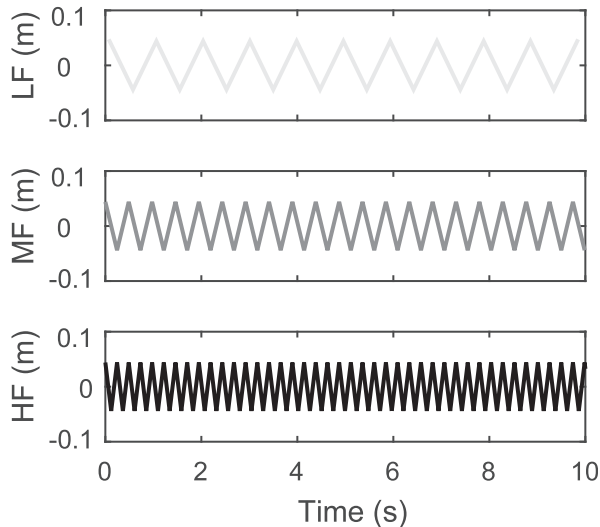


Figure 2. The three triangular viewpoint oscillation conditions. From top to bottom, *Low Frequency (LF; 1 Hz)*, *Medium Frequency (MF; 2 Hz)*, and *High Frequency (HF; 4 Hz)* conditions.

triangular shape, but the “natural” properties, in terms of the frequency and the period, were preserved.

High Frequency (HF): The *HF* condition was the same as the *MF* condition in terms of the shape of the oscillations, but the frequency was twice as high (4 s^{-1}) and the spatial period was twice as small (0.367 m).

Low Frequency (LF): The *LF* condition was the same as the *MF* condition but the frequency was twice as small (1 s^{-1}) and the spatial period (1.47 m) was twice as high.

Contrary to the *HF* and *LF* conditions, the *MF* condition involved real biological properties corresponding to what is called the walk ratio. The walk ratio is a human gait signature corresponding to the ratio between the step length and the step frequency (Sekiya & Nagasaki, 1998; Multon & Olivier, 2013). This ratio is invariable in most subjects in a large range of walking speeds. In the *MF* condition, its value is 0.367 m/steps per s. which is similar to the values recorded by Sekiya et al. (1998), where the walk ratio was 0.387 m/steps per s, whereas the value obtained here in the *HF* condition was significantly lower (0.092 m/steps per s) and that obtained in the *LF* condition was significantly higher (1.47 m/steps per s).

Experimental plan

The following experimental design was used in this study: 20 subjects were presented with 10 blocks of trials. In each block of 20 trials (five distances [6, 12, 18, 24, and 30 m] \times four optic flow conditions [*Linear*, *LF*, *MF*, and *HF*]), the order of the trials was chosen at random. The whole experiment lasted approximately 65 min per subject. This gave a total number of $20 \times 10 \times 4 \times 5 = 4,000$ observations and measurements of the dependent variable (the perceived distance traveled).

Data analysis

In each trial, independent variables (subject’s ID, block number, initial distance, and virtual simulation of self-movement condition) and the dependent variable (simulated traveled distance moved) were recorded. The simulated traveled distance moved by the subject was bounded by a start signal and a stop signal. Between these two signals, the tunnel advanced. The instantaneous simulated distance between the observer’s position and that of the target was recorded at a sampling frequency of 100 Hz.

Subjects’ estimates, as a function of the initial target distances under the four conditions of optic flow simulation, were adjusted (with Matlab fitting functions) using the leaky path integration model developed by Lappe et al. (2007).

In this model, the subjects monitor the current perceived distance $D(x)$ to the target during the movement as a function of their simulated position (x) and press the button when this distance becomes equal to zero. The instantaneous change in D with respect to x is given by

$$\frac{dD(x)}{dx} = -\alpha D - k \quad (1)$$

where k is the sensory gain ($k = 1$ in the case of an ideal observer) and α is the leaky integrator constant ($\alpha = 0$ in the case of an ideal observer). The general solution to this differential equation is

$$D(x) = \left(D_0 + \frac{k}{\alpha} \right) e^{-\alpha x} - \frac{k}{\alpha} \quad (2)$$

where D_0 is the actual initial distance to the target (before the subject starts moving). From this equation, we can obtain the distance traveled ($x(D_0)$) at which the subjects believed they had reached the target ($D = 0$), in the case of a given initial target distance (D_0):

$$x(D_0) = \frac{1}{\alpha} \ln \left(1 + \frac{\alpha D_0}{k} \right) \quad (3)$$

Statistical analyses

Shapiro-Wilks tests were used to check that the data were normally distributed. Once this condition was met, statistical analyses were conducted using repeated-measures analyses of variance (ANOVAs).

Results

Perceived distance traveled

When they were exposed to simulations inducing the feeling of forward movement toward a previously seen distant target, subjects indicated that they had reached

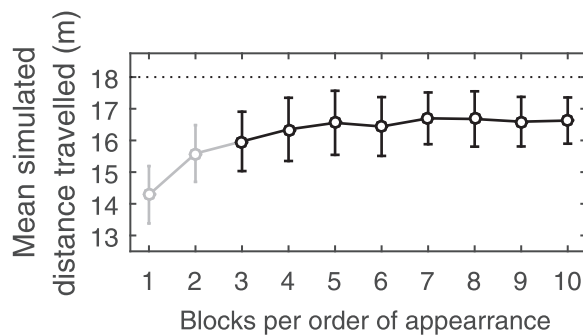


Figure 3. Mean simulated distance traveled per block of trials. Data points are means based on the performances of 20 subjects with the five target distances, and error bars give the standard errors of the means. A significant effect of the Block factor was observed, which disappeared when the analysis was restricted to the last eight blocks. The dotted line gives the average initial target distance.

the target after traveling on average only 89% of the initial target distance. An ANOVA was conducted on the simulated distance traveled at the moment when the subjects responded (the dependent variable). This analysis involved three independent variables ($\text{Block}_{10} \times \text{Distance}_5 \times \text{Optic_flow}_4$). It showed the existence of a main effect of the Block factor, $F(9, 171) = 5.377$, $p < 0.001$, $\eta_p^2 = 0.221$, and the Distance factor, $F(4, 76) = 257.311$, $p < 0.001$, $\eta_p^2 = 0.931$. It also showed the occurrence of an interaction between the Optic Flow and Distance factors, $F(12, 228) = 3.487$, $p < 0.001$, $\eta_p^2 = 0.155$, and between the Block and Distance factors, $F(36, 684) = 1.775$, $p < 0.005$, $\eta_p^2 = 0.085$.

In line with the results obtained by Bossard et al. (2016), subjects tended to give early responses more frequently in the first few experimental blocks, and their performances subsequently stabilized (Figure 3). Overall, it can be seen from Figure 3 that subjects tended to undershoot the simulated distance traveled. However, the presence of a Distance effect suggests the existence of a positive correlation between the initial target distance and the subject's distance traveled estimates. In the case of the largest distances, subjects undershot the simulated distance traveled: When the initial target was 30 m away, for example, the subjects responded after the simulated distance traveled was only 23 m on average. Conversely, with the shortest distances, subjects overshoot the simulated distance traveled. The interaction between Block and Distance factors shows a more pronounced block effect with large distances than with small distances. When the analysis was restricted to the last eight blocks, the block effect disappeared, $F(7, 133) = 1.195$, $p > 0.1$, $\eta_p^2 = 0.059$, and no interactions between Block and Distance factors were observed, $F(28, 532) = 1.336$, $p > 0.1$, $\eta_p^2 = 0.066$. However, the effect of the Distance factor, $F(4, 76) = 239.423$, $p < 0.001$, $\eta_p^2 =$

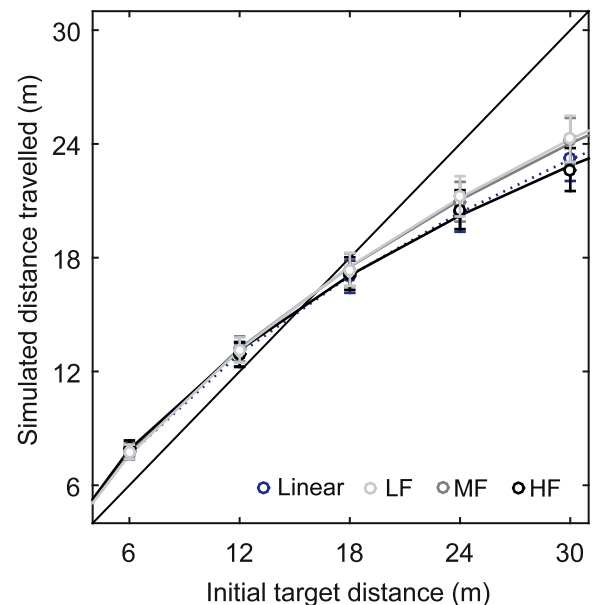


Figure 4. Distance traveled depending on the initial distance to the target in the *Linear*, *Low Frequency (LF)*, *Medium Frequency (MF)*, and *High Frequency (HF)* conditions. Data points are means based on eight repetitions carried out by each of the 20 subjects, and error bars give the standard errors of the means. The straight black line indicates the actual distances. Blue dotted ($k = 0.666$; $\alpha = 0.059$), light gray ($k = 0.688$; $\alpha = 0.055$), gray ($k = 0.687$; $\alpha = 0.055$), black ($k = 0.639$; $\alpha = 0.069$) lines are the fits obtained by fitting the average data to the leaky integration model (Lappe et al., 2007). See the Methods section for details.

0.926, and the effect of interactions between the Optic Flow and Distance factors persisted, $F(12, 228) = 2.801$, $p < 0.005$, $\eta_p^2 = 0.128$. Figure 4 shows the simulated distance traveled versus the distance to the previously seen static target under the four optic flow conditions (*Linear*, *HF*, *MF*, and *LF*). The existence of an interaction between these two factors means that the observers' responses depended in both cases on the distance factor but also that the latter factor contributed to the responses obtained via the optic flow factor. A post hoc test (Tukey's HSD test) was therefore performed, which showed that the *HF* condition differed significantly from the *MF* and *LF* conditions only at an initial distance to the target of 30 m (Figure 5). The subjects' perception of the distance traveled tended to be closer to the truth (slope of 1 between the initial target distance and the simulated distance traveled; see Figure 4) in the *LF* and *MF* conditions than in the *HF* conditions. This test also showed the existence of a significant difference between the *LF* and *Linear* conditions in the case of the longest initial distance to the target (30 m; Figure 5).

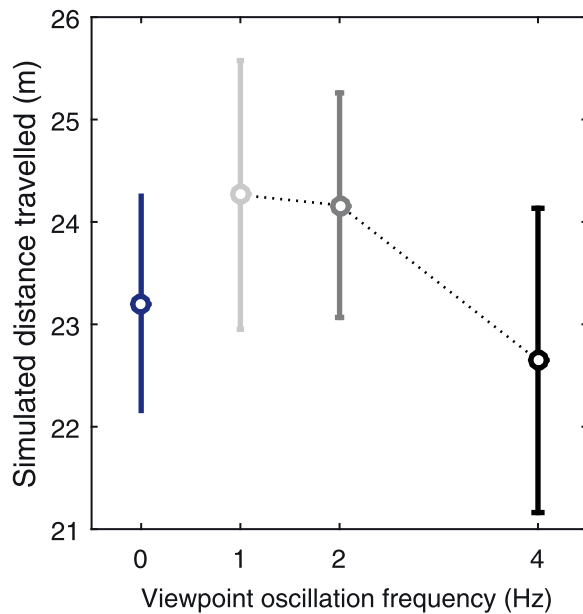


Figure 5. Distance traveled as a function of the oscillation frequency conditions with an initial distance of 30 m. Data points are means based on eight repetitions carried out by each of the 20 subjects, and error bars give the standard errors of the means.

The leaky path integrator model

Each subject's responses (in the range of initial distances tested) recorded in the four motion simulation conditions in the last eight last blocks of trials were adjusted using the leaky spatial integrator model developed by Lappe et al. (2007) to compute the sensory gain (k) and the leak rate (α). An ANOVA was performed on each of these values ($\text{Block}_8 \times \text{Optic_Flow}_4$). In the case of the gain parameter (k), no Block effect was found to occur, $F(7, 133) = 0.39$, $p > 0.5$, $\eta_p^2 = 0.02$ (Figure 6, Block 3 to Block 10), but the ANOVA on all 10 blocks showed the occurrence of a significant decrease in the value of the parameter k , $F(9, 171) = 2.441$, $p < 0.05$, $\eta_p^2 = 0.114$, in line with our previous studies (Bossard et al., 2016) and with the block effect observed in the case of the overall distance traveled (Figure 3). The sensory gain (k) in the last eight blocks of trials was also found to depend significantly on the Optic Flow factor, $F(3, 57) = 2.86$, $p < 0.05$, $\eta_p^2 = 0.131$, because Figure 7 shows that the value of k decreased at increasing oscillation frequencies. A Tukey's test showed that the k values differed significantly between the *HF* condition and the *MF* and *LF* conditions.

The second ANOVA ($\text{Block}_8 \times \text{Optic_Flow}_4$) showed that the leak rate (α) did not differ between blocks, $F(7, 133) = 2.05$, $p > 0.05$, $\eta_p^2 = 0.097$, but did differ between the Optic flow conditions, $F(3, 57) = 4.356$, $p < 0.01$, $\eta_p^2 = 0.187$ (Figure 7). The value of α increased with the oscillation frequencies. A Tukey's

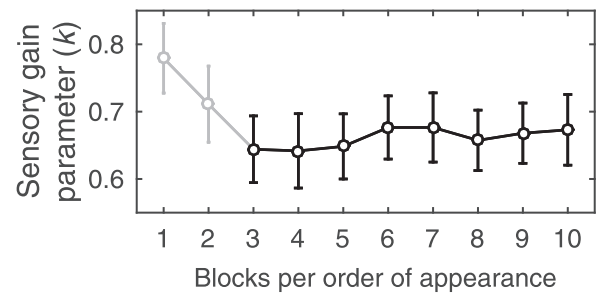


Figure 6. Mean sensory gain in the leaky spatial integrator model (k) depending on the experimental block. Data points are means based on 20 subjects, and error bars give the standard errors of the means.

test showed that the α values differed significantly between the *HF* condition and the *MF* and *LF* conditions.

Discussion

The aim of this study was to determine how various viewpoint oscillation frequencies (more or less close, in terms of frequency and spatial period, to the visual effects of vertical head oscillations during natural walking) may affect the subjects' perception of the distance traveled.

In addition to the global distance compression effect, which we found in a previous study (Bossard et al., 2016) to act in the same way in all four optic flow conditions studied, the main result obtained here

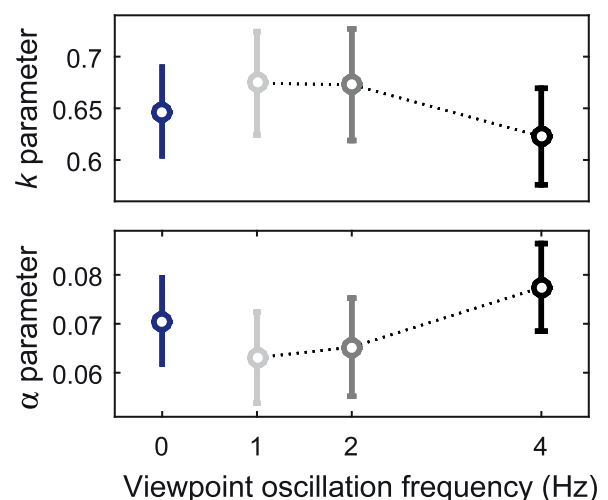


Figure 7. Values of the mean sensory gain (k) and the mean leak parameter (α) depending on the oscillation frequency in the last eight blocks. Optic flow conditions: *Linear* (0 Hz), *Low Frequency* (1 Hz), *Medium Frequency* (2 Hz), *High Frequency* (4 Hz). Data points are means based on the values of k or α computed on the last eight blocks of trials carried out by each of the 20 participants, and error bars give the standard errors of the means.

was that, whatever the value of the subjects' initial egocentric distance estimates, the spatiotemporal properties of the optic flow apparently modulated the path integration process, because differences in the subjects' perception of the distance traveled were observed, depending on the optic flow conditions. The results obtained in this study show that *LF* and *MF* conditions yielded more accurate distance traveled assessments than the *Linear* and *HF* conditions. The *LF* and *MF* conditions did not differ significantly, nor did the *HF* and *Linear* conditions (Figures 4 and 5). In other words, the subjects' perception of the distance traveled in this virtual environment tended to be closer to the truth in the *LF* and *MF* conditions than in the *HF* and *Linear* conditions. These results were confirmed by the parameters values of the leaky path integrator model, with which the sensory gain (k) was found to be significantly lower and the leak rate (α) significantly higher in the *HF* condition than the *LF* and *MF* conditions (Figure 7).

In agreement with the leaky path integrator model, in which it is assumed that a path's segments are integrated at every spatial step, we observe here that the k values tended to decrease and the α values, to increase with increasing viewpoint oscillation frequencies. This model partly explains the differences observed depending on the viewpoint oscillation frequency conditions applied. But the absence of any strong correlations between the model parameters and the oscillation frequency suggests that other parameters are probably involved in this process.

At this point, the question arises as to what exactly affected the subjects' self-motion perception in these various viewpoint oscillation frequency conditions. Observers are known, for example, to generate compensatory eye movements (ocular following responses) in response to the visual oscillation conditions to which they are subjected. Pursuit eye movements of this kind might indirectly stimulate the vestibular cortex in stationary subjects (Kim & Palmisano, 2008, 2010b; Hypothesis 3), which would lead to an improvement in the subjects' perception of self-motion. Conversely, in line with retinal motion hypothesis (Hypothesis 2), if subjects' eye movements do not differ between viewpoint oscillation frequency conditions, then the higher the viewpoint oscillation frequency, the higher the observer's global retinal motion will be. And as Palmisano and Kim (2009) have established, an increase in the retinal motion would result in a more compelling sensation of self-motion (in terms of the strength rating and the onset latency). This process would be beneficial in the present distance traveled estimation task, at least at *LF* and *MF* oscillation frequencies rather than the *Linear* condition. Conversely, the *HF* condition seems to have degraded the

subjects' performances, which suggests that the advantage of oscillations advantage might apply within specific limits.

To test Hypotheses 2 and 3, we therefore repeated the same basic experimental procedure, but this time, the eye movements and head motion were measured using electro-oculographic methods and the CAVE tracking system, respectively.

Experiment 2: EOG

Methods

Participants

Twelve participants (mean age 21 ± 4.3 , seven women and six men) with normal or corrected-to-normal vision took part in this experiment. They had no vestibular antecedents or disorders liable to affect their locomotor performances or their visual acuity. All the participants gave their written informed consent prior to the experiment, in keeping with the 1964 Helsinki Declaration, and the study was approved by the local ethics committee.

Apparatus

The laboratory setup and the virtual scene were identical to those used in Experiment 1.

Procedure

The procedure was practically identical to that used in Experiment 1, apart from the following three changes. First, the participants' head motions were recorded by the ART tracking system throughout the experiment at a sampling frequency of 100 Hz, and participants' vertical eye movements were monitored by EOG using a BIOPAC MP150 BioNomadix wireless system (Biopac Systems, Inc., Santa Barbara, CA) operating at a frequency of 1,000 Hz, with a ground electrode placed on the head in the middle of the frontal bone and four other EOG electrodes placed above and below each eye to record the vertical eye movements. The second change was the introduction of calibration phases, during which the observers had to fix a target (a cross) placed 12 m in front of them visually without moving their head. The cross oscillated vertically, at a frequency of 1 Hz and an amplitude of 1 m around each subject's eye level. At the same time, the cross approached the observers (which led to an increase in its size), until stopping 1.5 m in front of them. This phase was run five times before the experiment and once after every even-numbered block of trials. The third change was the addition of a

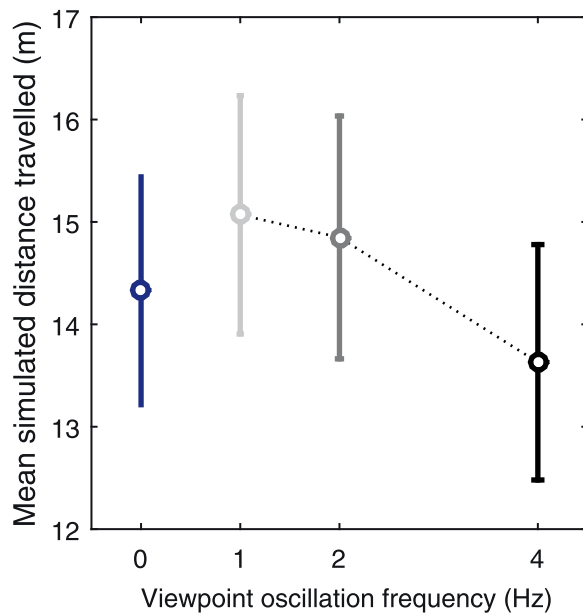


Figure 8. Mean distance traveled as a function of the oscillation frequency with the five initial distances. Data points are means based on seven repeated trials carried out by each of the 12 subjects, and error bars give the standard errors of the means.

supplementary block of trials at the end of the experiment, in which the target no longer disappeared. This final block was not included in the statistical analysis of the perceived distance traveled.

Experimental plan

The following experimental design was used here: 12 subjects were presented with eight blocks of 20 trials. In each block (five distances [6, 12, 18, 24, and 30 m] \times four optic flow conditions [*Linear*, *LF*, *MF*, and *HF*]), the order of the trials was chosen at random. The whole experiment lasted approximately 90 min per subject. This yielded a total number of $12 \times 8 \times 5 \times 4 = 1,920$ observations and measurements of the dependent variable (the perceived distance traveled).

Data analysis

A fast Fourier transformation (FFT) was performed on the raw data obtained in all the trials with the EOG system and the motion capture system. The area under the curve at frequencies of about 1, 2, and 4 Hz was then computed by integration with a step interval of ± 0.1 Hz.

Results

Perceived distance traveled

As in the first experiment, subjects gave their responses before reaching the position of the previously seen target.

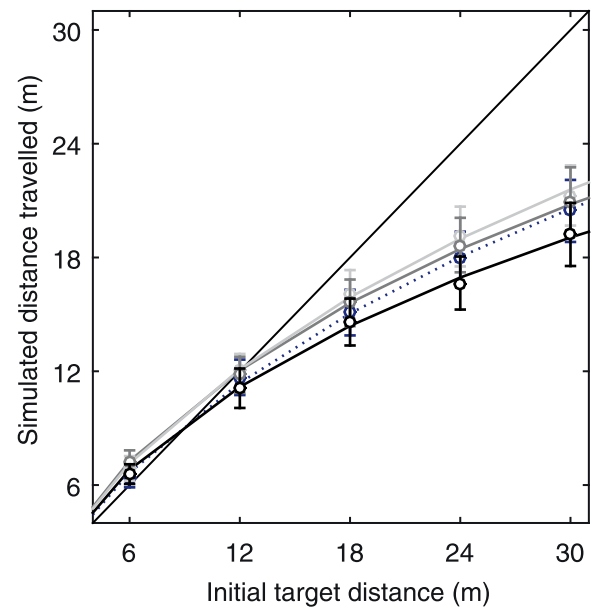


Figure 9. Distance traveled depending on the initial target distance in the *Linear* (*L*), *Low Frequency* (*LF*), *Medium Frequency* (*MF*), and *High Frequency* (*HF*) conditions. Data points are means based on eight repeated trials carried out by each of the 20 subjects, and error bars give the standard errors of the means. The black straight line indicates the actual distances. Blue dotted ($k = 0.78$; $\alpha = 0.087$), light gray ($k = 0.75$; $\alpha = 0.075$), gray ($k = 0.71$; $\alpha = 0.087$), and black ($k = 0.73$; $\alpha = 0.11$) lines are the fits obtained by fitting average data with the leaky integration model (Lappe et al., 2007). See the Methods section for details.

They pressed the button to indicate that they had reached the target after covering only 79% of the distance on average. Here again, there were significant differences between the effects of the optic flow conditions. Mean results are presented in Figure 8. An ANOVA showed the existence of a main effect of the Block factor, $F(7, 77) = 2.66$, $p < 0.05$, $\eta_p^2 = 0.195$; the Distance factor, $F(4, 44) = 166.03$, $p < 0.001$, $\eta_p^2 = 0.938$; and the Optic Flow factor, $F(3, 33) = 9.97$, $p < 0.001$, $\eta_p^2 = 0.475$. It also shows the occurrence of an interaction between the Optic Flow and Distance factors, $F(12, 132) = 2.09$, $p < 0.05$, $\eta_p^2 = 0.16$. A post hoc test (Tukey's HSD test) showed that the *HF* condition differed significantly from the *MF* and *LF* conditions (Figure 8).

As in the first experiment, subjects tended to give early responses more frequently in the first few blocks, and their performances subsequently stabilized. When the analysis was restricted to the last seven blocks, no block-related effects were observed, $F(6, 66) = 1.66$, $p > 0.1$, $\eta_p^2 = 0.131$, whereas the effects of the Optic Flow factor, $F(3, 33) = 9.41$, $p < 0.001$, $\eta_p^2 = 0.461$ (Figure 8) and the interaction between Optic Flow and Distance factors, $F(12, 132) = 1.92$, $p < 0.05$, $\eta_p^2 = 0.149$ (Figure 9) persisted.

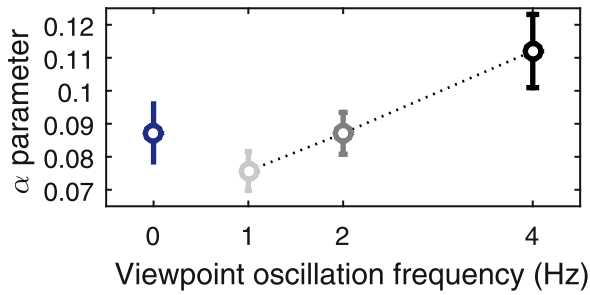


Figure 10. Mean leak parameter values (α) depending on the oscillation frequency in the last seven blocks of trials. Optic flow conditions: *Linear* (0 Hz), *Low Frequency* (1 Hz), *Medium Frequency* (2 Hz), *High Frequency* (4 Hz). Data points are means based on the α values computed on the last seven blocks carried out by each of the 12 participants, and error bars give the standard errors of the means.

Leaky path integrator model

As far as the model parameters were concerned, as in the first experiment, an effect of the Block factor on the k values was found to occur, $F(7, 77) = 2.75, p < 0.05, \eta_p^2 = 0.2$, and this effect disappeared when only the last seven blocks were analyzed, $F(6, 66) = 1.23, p > 0.05, \eta_p^2 = 0.102$. Again, in the last seven blocks, an effect of the Optic Flow on the α values, $F(3, 33) = 2.83, p < 0.05, \eta_p^2 = 0.245$ (Figure 10) was found to occur: The value of α

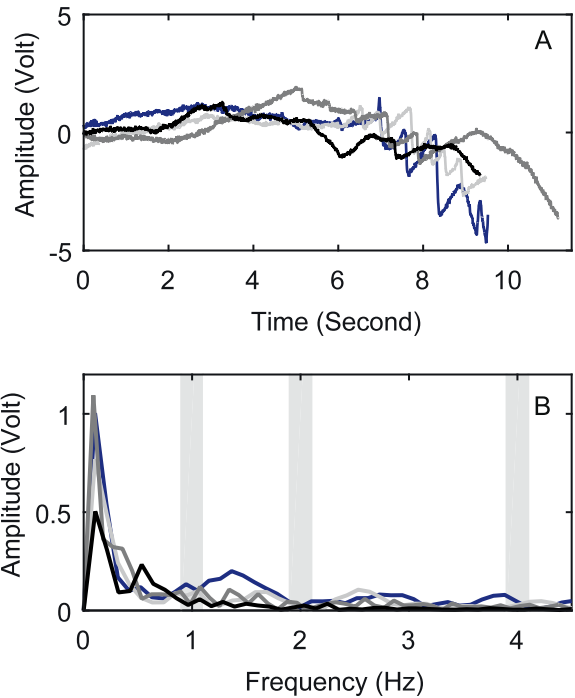


Figure 12. (A) Raw EOG data obtained in the experimental phases for one participant, corresponding to one trial in each optic flow condition: *Linear* (blue), *Low Frequency* (light gray), *Medium Frequency* (gray), *High Frequency* (dark gray). (B) Spatial-frequency content of the previous signals. The light blue areas are the three areas that will be used to compare the spatial-frequency content of all the experimental trials.

increased with the oscillation frequency. A Tukey’s test showed that the α values observed in the *HF* condition differed significantly from those recorded in the *MF* and *LF* conditions.

Eye movements

In all the calibration data, we first analyzed the spatial-frequency content by calculating 2D FFTs on raw EOG data. These data showed that observers were able to pursue the oscillating target (the cross) visually when it was oscillating at a frequency of 1 Hz (Figure 11). Logically, EOG signals increased in amplitude as the oscillating target came closer.

In all the trials conducted in the experimental phases, we analyzed the eye movements’ spatial-frequency content by calculating 2D FFTs on the EOG data obtained. The area under the curve around frequencies of 1, 2, and 4 Hz was then computed by integration, with a step interval of ± 0.1 Hz (Figure 12B, gray area).

An ANOVA was then conducted on the values of the areas under the curve, one at each frequency of interest (1, 2, and 4 Hz), denoted the value of observation (VoO) in the following figures (Figure 12). This analysis involved three independent variables (VoO₃ × Dis-

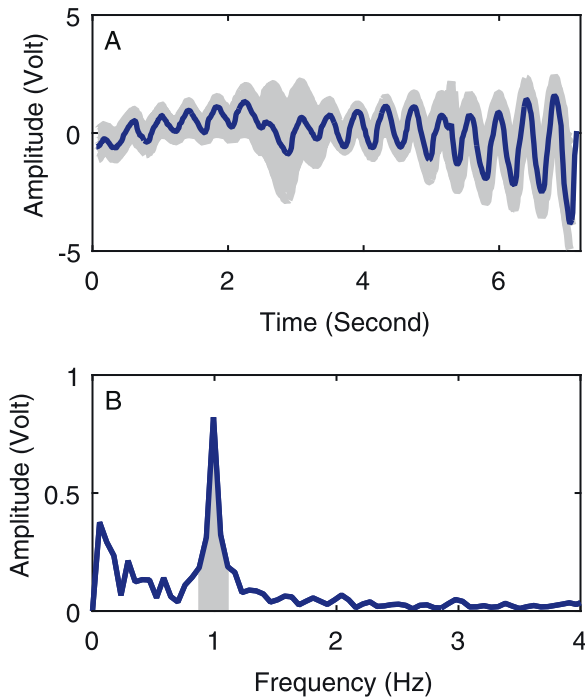


Figure 11. (A) Mean EOG raw data recorded during the calibration phases for one participant. (B) Spatial-frequency content of the previous signal. The gray surface is an example of the area that will be used to compare the spatial-frequency contents of all the experimental trials.

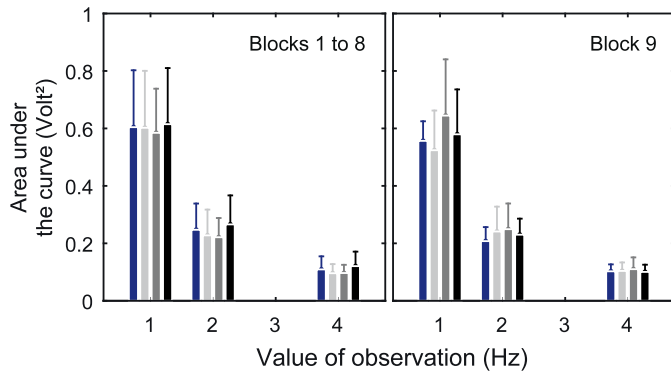


Figure 13. Mean values of the area under the curve of the spatial-frequency content in the case of eye movements around 1, 2, and 4 Hz, depending on Optic Flow condition (*Linear*, *Low*, *Medium*, and *High*) in the first eight blocks of trials (left) and the ninth block, when the target was visible (on the right).

tance₅ × Optic_Flow₄). The results obtained here showed that the main effects involved were those of the Value of Observation factor, $F(2, 22) = 38.7$, $p < 0.001$, $\eta_p^2 = 0.779$, and the Distance factor, $F(4, 44) = 6.4$, $p < 0.001$, $\eta_p^2 = 0.367$. An interaction was also found to occur between the Value of Observation and the Distance factors, $F(8, 88) = 4.2$, $p < 0.001$, $\eta_p^2 = 0.276$.

The effect of the Value of Observation factor, which was supported by a Tukey's test, indicates that there was a greater spatial-frequency content around 1 Hz than with the other two values of observation. The effect of the Distance factor indicates the existence of a negative correlation between the area under the curve and the distance to be estimated by the subjects. And the presence of an interaction means that the effect of one factor varied depending on the modalities involved in the other factor. These effects were mainly due to the task: Participants tracked the target with their eyes and their head, which led the signal to drift increasingly as they were approaching the target. The effect of the Distance factor was due to the fact that this drift occupied a larger proportion of the signal at shorter distances than at longer distances. The effect of the Value of Observation can be explained by the weakness of this drift because it created mainly low frequencies (up to 1 Hz) rather than high frequencies.

One of the main results obtained here was the absence of any effect of the Optic Flow factor, $F(3, 33) = 1.9$, $p > 0.1$, $\eta_p^2 = 0.148$ (Figure 13, Block 1 to 8). This means that the various Optic Flow conditions did not involve different compensatory eye movements.

The ninth block of trials, when the target no longer disappeared, was used to test whether the presence or absence of the target led to any change in the eye movements. The same analyses were performed as above, and the ANOVA showed that the main effect involved was that of the Value of Observation factor, $F(2, 22) = 55.9$, $p < 0.001$, $\eta_p^2 = 0.836$ (Figure 13).

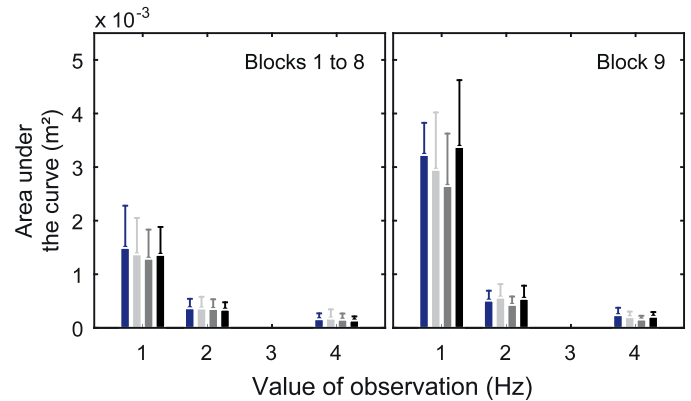


Figure 14. Mean areas under the curves of the spatial-frequency content in the case of head movements at frequencies of around 1, 2, and 4 Hz, depending on the Optic Flow condition (*Linear*, *Low*, *Medium*, and *High*) in the first eight blocks of trials (left) and the ninth block, when the target was visible (on the right).

Head movements

This same analysis was performed on the head movements and gave similar results (Figure 14) to those observed in the case of eye movements. In the first eight blocks of trials, the results showed that the main effects involved were those of the Value of Observation factor, $F(2, 22) = 23.9$, $p < 0.001$, $\eta_p^2 = 0.686$, and the Distance factor, $F(4, 44) = 6.68$, $p < 0.001$, $\eta_p^2 = 0.378$. A significant interaction was also found to occur between the Value of Observation and the Distance factors, $F(8, 88) = 6.63$, $p < 0.001$, $\eta_p^2 = 0.376$.

The analysis conducted on the ninth block of trials showed similar effects of the Value of Observation factor, $F(2, 22) = 14.5$, $p < 0.001$, $\eta_p^2 = 0.568$ (Figure 14); the Distance factor, $F(4, 44) = 6.22$, $p < 0.001$, $\eta_p^2 = 0.361$; and the occurrence of an interaction between the Value of Observation and Distance factors, $F(8, 88) = 5.7$, $p < 0.001$, $\eta_p^2 = 0.341$.

Discussion

The aim was to determine whether subjects generated compensatory eye and/or head movements when they were subjected to viewpoint oscillations, and if so, whether these eye and/or head movements differed depending on the viewpoint oscillation frequency.

The results obtained on the subjects' distance traveled estimations were similar to those obtained in the first experiment: The Block and Distance factors had similar effects, and a similar interaction between the Optic Flow and Distance factors was found to occur. In addition, a main effect of Optic Flow factor was observed: The subjects' estimates recorded in the *HF* condition differed significantly from those obtained in the *MF* and *LF* conditions (Figure 8).

In terms of eye and head movements, no significant differences were detected between the four viewpoint conditions, and no evidence was therefore obtained that eye or head pursuit movements were associated with the various oscillation frequencies. These results may be due to the fact that participants tracked the memorized position of the previously seen target on the nontextured ground. Indeed, as Palmisano et al. (2012) previously reported, the observers' eyes were almost stationary and did not oscillate in response to a simulated viewpoint oscillation when they had to gaze at a stationary fixation point. Based on these results, we concluded that increasing the viewpoint oscillation frequency results in an increase in the global retinal flow (hypothesis 2). In line with the latter hypothesis, Palmisano et al. (2012) showed that an increasing retinal motion results in a more compelling sensation of vection: The subjects' vection strength ratings increased with the simulated viewpoint oscillations in comparison to what occurred with no oscillations, and the vection strength also increased with the oscillation frequency (which increases the global retinal motion).

At this point, it is worth noting that simply adding more global retinal motion to a visually simulation of forward self-motion does not always improve subjects' self-motion perception: The results of Experiment 1 and Experiment 2 suggest that adding global retinal motion can be either beneficial (in *LF* and *MF* conditions) or detrimental (in the *HF* condition) to the perception of the distance traveled, in comparison with the *Linear* condition. *LF* and *MF* conditions give more accurate estimates of the distance traveled than the *HF* condition.

Lastly, it is possible that the benefits of simulated viewpoint oscillation (in addition to the global retinal motion hypothesis) may also be partly due to the fact that it evokes in participants similar visual effects of head movements to those perceived during walking or running (Bubka & Bonato, 2010). To test this hypothesis (Hypothesis 4), we therefore conducted a third experiment in which subjects were subjected to two viewpoint oscillation conditions inducing equivalent global retinal motion. The first condition was a pattern having similar characteristics to those of the patterns generated by actual walking, and the second condition involved a pattern that was not biologically realistic.

Experiment 3

Participants

Ten participants, who were university students (mean age 25 ± 4.9 , six men and four women),

participated in exchange for course credits. They all had normal or corrected-to-normal vision and no vestibular antecedents or disorders. All the participants gave their written informed consent prior to the experiment, in keeping with the 1964 Helsinki Declaration, and the study was approved by the local ethics committee.

Apparatus

The laboratory, the virtual reality device, and the virtual scene were all identical to those used in Experiment 2.

Procedure

Conditions of virtual simulation of self-motion: the optic flow factor

Bio-coherent: In the bio-coherent condition, a linear translation was imposed on the subject's viewpoint (via a virtual camera), combined with vertical triangular oscillations with a frequency of 2 Hz, corresponding to the visual effects of the step frequency, and horizontal triangular oscillations at a frequency of 1 Hz, corresponding to the visual effects of the stride frequency. The speed in depth was $1.47 \text{ m}\cdot\text{s}^{-1}$, as in the conditions applied in Experiments 1 and 2.

Bio-incoherent: This condition was the same as the previous one, but with vertical triangular oscillations at a frequency of 1 Hz and horizontal triangular oscillations at a frequency of 2 Hz.

These two conditions created an identical amount of visual motion relative to the observer.

Experimental design

The following experimental design was used here: 10 subjects were presented with 10 blocks of 10 trials. In each block of trials (five distances [6, 12, 18, 24, and 30 m] \times two optic flow conditions [bio-coherent and bio-incoherent]), the order of the trials was chosen at random. The whole experiment lasted approximately 45 min per subject. This yielded a total number of $10 \times 10 \times 5 \times 2$ or 1,000 observations and measurements of the dependent variable (the perceived distance traveled).

Results

Perceived distance traveled

As in the two first experiments, subjects gave their responses before reaching the position of the previously seen target. They pressed the button to indicate that

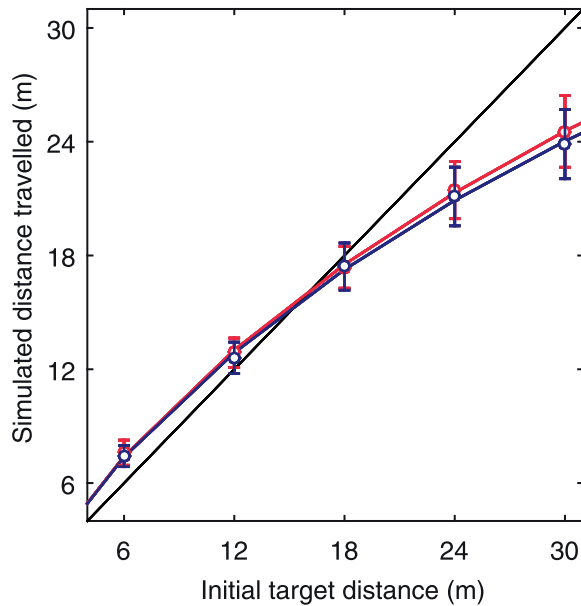


Figure 15. Distance traveled depending on the initial target distance in the bio-coherent and bio-incoherent conditions. Data points are means based on eight repeated trials carried out by each of the 10 subjects, and error bars give the standard errors of the means. The straight black line indicates the actual distances. Red ($k = 0.69$; $\alpha = 0.043$) and blue ($k = 0.68$; $\alpha = 0.046$) lines are the fits obtained by fitting the average data to the leaky integration model (Lappe et al., 2007).

they had reached the target after covering only 90.7% of the distance on average. An ANOVA showed the existence of a main effect of the Block factor, $F(9, 81) = 3.06$, $p < 0.005$, $\eta_p^2 = 0.254$, and the Distance factor, $F(4, 36) = 100.78$, $p < 0.001$, $\eta_p^2 = 0.918$, but no effect of the Optic Flow factor was observed, $F(1, 9) = 3.08$, $p > 0.05$, $\eta_p^2 = 0.255$, and no interaction between the Optic Flow and Distance factors was found to occur, $F(4, 36) = 1.9$, $p > 0.05$, $\eta_p^2 = 0.173$ (Figure 15). In line with the two first experiments, subjects tended to give early responses more frequently in the first few blocks, and their performances subsequently stabilized. When the analysis was restricted to the last nine blocks, no block-related effects were observed, $F(8, 72) = 2$, $p > 0.05$, $\eta_p^2 = 0.182$.

Leaky path integrator model

As far as the model parameters were concerned, as in the two first experiments, an effect of Block factor on the k values was found to occur, $F(9, 81) = 5.62$, $p < 0.001$, $\eta_p^2 = 0.384$, and this effect disappeared when only the last nine blocks were analyzed, $F(8, 72) = 1.67$, $p > 0.05$, $\eta_p^2 = 0.156$. No effect of the Optic Flow factor on the k values, $F(1, 9) = 0.12$, $p > 0.05$, $\eta_p^2 = 0.012$, or the α values, $F(1, 9) = 0.45$, $p > 0.05$, $\eta_p^2 = 0.047$, was found to occur.

Discussion

The fourth hypothesis focused on the idea that viewpoint oscillation taps into the visual processes normally used to perceive self-motion based on the natural optic flow patterns that occur during walking. Consistent with this hypothesis, various studies (Kokinara, Kiltner, Blom, & Slater, 2016; Lécuyer, Burkhardt, Henaff, & Donikian, 2006; Terziman, Lécuyer, Hillaire, & Wiener, 2009; Terziman, Marchal, Multon, Arnaldi, & Lécuyer, 2013) have reported that combining the translational optic flow with simulated head oscillations during virtual displacements enhances the observer's sensation of walking. This feeling of walking may increase the sense of presence in a virtual environment (Interrante, Ries, Lindquist, Keating, & Anderson, 2008). Bubka and Bonato (2010) have proposed an ecological explanation for these findings, based on the possible advantages of viewpoint oscillation for vection, due to the fact that the resulting retinal flow patterns are similar to those generated by actual walking and therefore trigger self-motion perception, which improves path integration and the subjects' distance traveled assessments (Bossard et al., 2016; Palmisano et al., 2011). On the other hand, as Palmisano et al. established in 2014, when observers are presented with a playback of a viewpoint oscillation corresponding to their own head movements when walking on the spot ("less ecological") or when walking on a treadmill walking ("more ecological"), no differences were found between these two conditions. In this experiment, similar results were obtained: No differences were observed between the bio-coherent and bio-incoherent conditions. These results support the second hypothesis, according to which the amount of global retinal motion plays an important role in visual self-motion perception.

General discussion

In these experiments, a virtual reality setup (the CAVE system) was used to make stationary observers perform a distance traveled estimation task. This device made it possible to isolate the optic flow from the other main sources of information (vestibular and proprioceptive inputs). The data obtained were fitted with the leaky path integration model (Lappe et al., 2007), which yielded further information about the path integration process. Observers performing a distance traveled estimation task were presented with various optic flow conditions simulating forward self-motion.

When they were exposed to simulations inducing the feeling of forward movement toward a previously seen distant target, subjects indicated that they had reached

the target after traveling only 86% on average of the distance to the target (Experiment 1: 89%; Experiment 2: 79%; and Experiment 3: 90%). Also, subjects tended to go beyond the target in the case of short distances and to undershoot it in that of large distances, which is consistent with the results obtained in previous studies using the same procedure (Bossard et al., 2016; Harris et al., 2012; Redlick et al., 2001). These results are in agreement on the whole with those obtained in several studies on the perceptual compression of large distances in the real world on the basis of static visual cues (Loomis, Da Silva, Fujita, & Fukushima, 1992), as well as in virtual environments (Thompson et al., 2003; Mohler, Thompson, & Creem-Regehr, 2006). This phenomenon was found to be generally more pronounced in virtual environments (Knapp & Loomis, 2004; Loomis & Knapp, 2003; Piryankova, De La Rosa, Kloos, Bühlhoff, & Mohler, 2013). However, the subjects' underestimation of egocentric distance does not account for the systematically differential effects or our optic flow conditions on their assessment of the distance traveled: Regardless of their initial egocentric distance estimates, adding viewpoint oscillatory components was found to affect their perception of the distance traveled.

The aim of this study was to compare the perception of distance traveled induced by various oscillating viewpoint conditions to test four hypotheses frequently mentioned in the literature. The aim of the first experiment was to determine whether various viewpoint oscillation frequencies might affect subjects' distance traveled perception and, if so, whether this may be attributable to the path integration process. The second experiment was intended to test whether viewpoint oscillations may generate pursuit eye movements, which would indirectly stimulate the vestibular cortex in stationary subjects (Hypothesis 3) or whether these oscillations might generate a more global pattern of retinal motion (Hypothesis 2). The outcome in both cases would be to increase the sensation of self-motion. The third experiment focused on the ecological explanation for the benefits of viewpoint oscillation.

In Experiment 1, participants were subjected to four optic flow conditions simulating forward self-motion. The first condition involved a purely translational optic flow with a constant speed, whereas the other three flow conditions were based on vertical triangular oscillations at three different frequencies (1, 2, and 4 Hz) in addition to the previous sensation of linear forward motion. The results obtained showed that in the *HF* condition, participants responded earlier than in the *LF* and *MF* conditions. The greater viewpoint frequency therefore seems to have led the participants to overestimate the distance traveled more conspicuously (i.e., to undershooting the target more greatly). Assuming the distance traveled assessment to be part of

the path integration process whereby short sections of a movement are integrated, yielding the total path (Maurer & Séguinot, 1995; Mittelstaedt & Mittelstaedt, 1973), we fitted our data to the leaky path integrator model developed by Lappe et al. (2007) to explain the differences observed under various viewpoint oscillation conditions. The parameters of the model were found to be different in the *HF* condition compared with the *LF* and *MF* conditions. The sensory gain (k) was significantly lower in the *HF* condition than in the *LF* and *MF* conditions, and the leak rate (α) was significantly larger (Figure 7). Although the k values tended to decrease and the α values tended to increase with increasing viewpoint oscillation frequencies, the absence of any strong correlations between the model parameters and the increase in the oscillation frequency suggest that other parameters are probably involved in this process. In addition, the results obtained in the *Linear* condition did not correlate with those obtained in the other conditions. This condition therefore does not seem to be equivalent to a viewpoint oscillating at 0 Hz but a particular condition apart, which again seems to indicate that other processes might be involved.

This difference between the *Linear* condition estimates and the other conditions argues against the possible explanation suggested by Palmisano et al. (2011), that the viewpoint jitter advantage of self-motion may be that it makes the simulated environment appear more 3D. In this approach, the increase in the viewpoint oscillation frequency may add further motion parallax cues to the layout of the simulated 3D environment, and the three viewpoint oscillation conditions should give better distance traveled estimates than the *Linear* condition.

In Experiment 2, we repeated the first experiment while measuring the subjects' eye and head movements in order to test Hypotheses 2 and 3. The distance traveled estimates and the values of the model parameters values were similar to those obtained in Experiment 1. The main result obtained in this experiment was the absence of obvious differences between the four viewpoint conditions in terms of the subjects' eye and head movements. Thus, for this experiment, we appear to be able to rule out Hypothesis 3, according to which viewpoint oscillation might generate pursuit eye movements indirectly stimulating the vestibular cortex of stationary subjects (Kim & Palmisano, 2008), which might in turn increase the sensation of self-motion. On the other hand, these results show that viewpoint oscillation increases the global retinal flow in comparison with *Linear* conditions and that the increase in the oscillation frequency leads to an increase in the global retinal motion. In line with the retinal motion hypothesis (Hypothesis 2), which suggests that an increase in the global retinal motion might strengthen the sensation of self-motion,

the results of Experiments 1 and 2 show that the participants tended to estimate the distance traveled more accurately when they were exposed to *LF* and *MF* conditions than to the *Linear* condition, whereas when more retinal motion occurred in the *HF* condition, participants give less accurate distance traveled estimates. At this point, the third experiment was designed to test whether the benefits of simulated viewpoint oscillation might be restricted to a range of frequencies inducing in the participants similar visual effects to those of head movements triggered during walking, which might tap into the visual processes normally involved in the perception of self-motion (Bubka & Bonato, 2010; Lécuyer et al., 2006; Palmisano et al., 2014; Hypothesis 4). In Experiment 3, the two conditions of simulated viewpoint oscillation induced the same amount of visual motion (and hence the same amount of global retinal motion), but one of them was based on a pattern resembling the visual effects of natural walking (the bio-coherent condition) and the other on a biologically unrealistic pattern (the bio-incoherent condition). The ecological hypothesis predicts that the bio-coherent condition is likely to improve the subjects' perception of the distance traveled. Contrary to this prediction, subjects gave similar responses in both of these two conditions.

All in all, these findings seem to support the hypothesis that greater global retinal motion strengthens the sensation of self-motion. However, they also suggest that there exists a range of frequencies in which the benefits to distance traveled perception are expressed. Palmisano et al. (2012) reported that subjects' vection strength ratings increased with the simulated viewpoint oscillation frequencies (which increase the global retinal motion), and Kim and Palmisano (2008) have shown the existence of a strong positive correlation between subjects' vection speed ratings and vection strength ratings during forward vection. In addition, Apthorp and Palmisano (2014) have established in a psychophysical study that the perceived speed increased when a radially expanding flow contained a 2-Hz vertically oscillating component in comparison with a smooth in-depth stimulus. In several studies, Palmisano and his colleagues have suggested that viewpoint jitter may have improved subjects' self-motion perception in depth by introducing path errors (Palmisano et al., 2011). These errors would increase the observers' perceived speed of self-motion in depth with the increasing viewpoint oscillation frequency. Further studies are now required to test this possible explanation.

In conclusion, simulated viewpoint oscillations seem to enhance subjects' sensation of self-motion within a certain range of frequencies, which improves their estimates of the distances traveled. However, beyond this 2-Hz range or so, subjects' overestimation of their

simulated self-motion speed perception might explain why they underestimated the distance required to reach the previously seen target in the *HF* condition but not in the *LF* and *MF* conditions. This hypothesis will have to be tested in a future study.

Conclusion

These three experiments show that viewpoint oscillation frequency influences static observers' distance traveled perception. More specifically, *LF* (1 Hz) and *MF* (2 Hz) conditions improved the subjects' distance traveled assessments, and no significant differences were detected between these two conditions. A high oscillation frequency of 4 Hz deteriorated their performances, however. The second experiment shows that these effects were not here generated by pursuit eye movements, which would have stimulated the vestibular cortex indirectly: The main cause responsible for the improved performances observed in the first two conditions seems to have been the increase in the global retinal motion.

Keywords: self-motion, optic flow, distance traveled, global retinal motion, path integration

Acknowledgments

This study was supported by a doctoral fellowship awarded to Martin Bossard (French Ministry of Higher Education and Research). We wish to thank Cédric Goulon and Jean-Claude Lepecq for their assistance with these experiments, Remy Casanova for his comments on the data, the CRVM team (Pierre Mallet and Jean-Marie Pergandi) for helping to make this study possible, and Jessica Blanc for correcting and improving the English manuscript.

Commercial relationships: none.

Corresponding author: Martin Bossard.

Email: martin.bossard@univ-amu.fr.

Address: Aix-Marseille Univ, CNRS, ISM, Marseille, France.

References

- Apthorp, D., & Palmisano, S. (2014). The role of perceived speed in vection: does perceived speed modulate the jitter and oscillation advantages? *PLoS One*, *9*, e92260.
- Ash, A., & Palmisano, S. (2012). Vection during

- conflicting multisensory information about the axis, magnitude, and direction of self-motion. *Perception*, *41*, 253–267.
- Bossard, M., Goulon, C., & Mestre, D. R. (2016). Viewpoint oscillation improves the perception of distance travelled based on optic flow. *Journal of Vision*, *16*(15):4, doi:10.1167/16.15.4. [PubMed] [Article]
- Brandt, T., Bartenstein, P., Janek, A., & Dieterich, M. (1998). Reciprocal inhibitory visual-vestibular interaction: Visual motion stimulation deactivates the parieto-insular vestibular cortex. *Brain*, *121*, 1749–1758.
- Bremmer, F., & Lappe, M. (1999). The use of optical velocities for distance discrimination and reproduction during visually simulated self-motion. *Experimental Brain Research*, *127*, 33–42.
- Bubka, A., & Bonato, F. (2010). Natural visual-field features enhance vection. *Perception*, *39*, 627–635.
- Campos, J. L., Butler, J. S., & Bühlhoff, H. H. (2012). Multisensory integration in the estimation of walked distances. *Experimental Brain Research*, *218*, 551–565.
- Campos, J. L., Butler, J. S., & Bühlhoff, H. H. (2014). Contributions of visual and proprioceptive information to travelled distance estimation during changing sensory congruencies. *Experimental Brain Research*, *232*, 3277–3289.
- Chrastil, E. R., & Warren, W. H. (2012). Active and passive contributions to spatial learning. *Psychonomic Bulletin & Review*, *19*, 1–23.
- Cruz-Neira, C., Sandin, D. J., & DeFanti, T. A. (1993). Surround-screen projection-based virtual reality: The design and implementation of the CAVE. In *Proceedings of the 20th annual conference on computer graphics and interactive techniques (SIGGRAPH '93)* (pp. 135–142). New York: ACM.
- Denton, G. G. (1980). The influence of visual pattern on perceived speed. *Perception*, *9*, 393–402.
- Dichgans, J., & Brandt, T. (1978). Visual-vestibular interaction: Effects on self-motion perception and postural control. In R. Held, H. Leibowitz, & H.-L. Teuber (Eds.), *Handbook of sensory physiology* (Vol. 8, pp. 755–804). New York: Springer.
- Durgin, F. H. (2009). When walking makes perception better. *Current Directions in Psychological Science*, *18*, 43–47.
- Durgin, F. H., Akagi, M., Gallistel, C. R., & Haiken, W. (2009). The precision of locomotor odometry in humans. *Experimental Brain Research*, *193*, 429–436.
- Durgin, F. H., Gigone, K., & Scott, R. (2005). Perception of visual speed while moving. *Journal of Experimental Psychology: Human Perception and Performance*, *31*, 339.
- Esch, H., & Burns, J. (1996). Distance estimation by foraging honeybees. *Journal of Experimental Biology*, *199*, 155–162.
- Frenz, H., & Lappe, M. (2005). Absolute travel distances from optic flow. *Vision Research*, *45*, 1679–1692.
- Gibson, J. J. (1950). *The perception of the visual world*. Boston: Houghton-Mifflin.
- Grüsser, O. J., Pause, M., & Schreier, U. (1990). Localization and responses of neurones in the parieto-insular vestibular cortex of awake monkeys (*Macaca fascicularis*). *Journal of Physiology*, *430*, 537–557.
- Harris, L. R., Herpers, R., Jenkin, M., Allison, R. S., Jenkin, H., Kapralos, B., . . . Felsner, S. (2012). The relative contributions of radial and laminar optic flow to the perception of linear self-motion. *Journal of Vision*, *12*(10):7, 1–10, <http://www.journalofvision.org/content/12/10/7>, doi:10.1167/12.10.7. [PubMed] [Article]
- Harris, L. R., Jenkin, M., & Zikovitz, D. C. (2000). Visual and non-visual cues in the perception of linear self-motion. *Experimental Brain Research*, *135*, 12–21.
- Harris, L. R., Jenkin, M. R., Zikovitz, D., Redlick, F., Jaekl, P., Jasiobedzka, U. T., . . . Allison, R. S. (2002). Simulating self-motion I: Cues for the perception of motion. *Virtual Reality*, *6*(2), 75–85.
- Interrante, V., Ries, B., Lindquist, J., Keading, M., & Anderson, L. (2008). Elucidating factors that can facilitate veridical spatial perception in immersive virtual environments. *Presence: Teleoperators and Virtual Environments*, *17*, 176–198.
- Israël, I., & Berthoz, A. (1989). Contribution of the otoliths to the calculation of linear displacement. *Journal of Neurophysiology*, *62*, 247–263.
- Kearns, M. J., Warren, W. H., Duchon, A. P., & Tarr, M. J. (2002). Path integration from optic flow and body senses in a homing task. *Perception*, *31*, 349–374.
- Kim, J., Chung, C. Y., Nakamura, S., Palmisano, S., & Khoo, S. K. (2015). The Oculus Rift: A cost-effective tool for studying visual-vestibular interactions in self-motion perception. *Frontiers in Psychology*, *6*, 248.
- Kim, J., & Khoo, S. (2014). A new spin on vection in depth. *Journal of Vision*, *14*(5):5, 1–10, <http://www.journalofvision.org/content/14/5/5>, doi:10.1167/14.5.5. [PubMed] [Article]

- Kim, J., & Palmisano, S. (2008). Effects of active and passive viewpoint jitter on vection in depth. *Brain Research Bulletin*, *77*, 335–342.
- Kim, J., & Palmisano, S. (2010a). Eccentric gaze dynamics enhance vection in depth. *Journal of Vision*, *10*(12):7, <http://www.journalofvision.org/content/10/12/7>, doi:10.1167/10.12.7. [PubMed] [Article]
- Kim, J., & Palmisano, S. (2010b). Visually mediated eye movements regulate the capture of optic flow in self-motion perception. *Experimental Brain Research*, *202*, 355–361.
- Kim, J., Palmisano, S., & Bonato, F. (2012). Simulated angular head oscillation enhances vection in depth. *Perception*, *41*, 402–414.
- Knapp, J. M., & Loomis, J. M. (2004). Limited field of view of head-mounted displays is not the cause of distance underestimation in virtual environments. *Presence*, *13*, 572–577.
- Kokkinara, E., Kilteni, K., Blom, K. J., & Slater, M. (2016). First person perspective of seated participants over a walking virtual body leads to illusory agency over the walking. *Scientific Reports*, *6*, 28879.
- Lappe, M., Bremmer, F., & Van den Berg, A. V. (1999). Perception of self-motion from visual flow. *Trends in Cognitive Sciences*, *3*, 329–336.
- Lappe, M., Jenkin, M., & Harris, L. R. (2007). Travel distance estimation from visual motion by leaky path integration. *Experimental Brain Research*, *180*, 35–48.
- Lécuyer, A., Burkhardt, J. M., Henaff, J. M., & Donikian, S. (2006). Camera motions improve sensation of walking in virtual environments. *Proceedings of IEEE Virtual Reality*, 11–18.
- Loomis, J. M., Da Silva, J. A., Fujita, N., & Fukusima, S. S. (1992). Visual space perception and visually directed action. *Journal of Experimental Psychology: Human Perception and Performance*, *18*, 906.
- Loomis, J. M., & Knapp, J. M. (2003). Visual perception of egocentric distance in real and virtual environments. *Virtual and Adaptive Environments*, *11*, 21–46.
- Maurer, R., & Séguinot, V. (1995). What is modelling for? A critical review of the models of path integration. *Journal of Theoretical Biology*, *175*, 457–475.
- Mittelstaedt, H., & Mittelstaedt, M. L. (1973). Mechanismen der Orientierung ohne richtende Außenreize [Mechanisms of orientation without orienting external stimuli]. *Fortschritte der Zoologie*, *21*, 46–58.
- Mittelstaedt, M. L., & Mittelstaedt, H. (1980). Homing by path integration in a mammal. *Naturwissenschaften*, *67*, 566–567.
- Mittelstaedt, M. L., & Mittelstaedt, H. (2001). Idiothetic navigation in humans: Estimation of path length. *Experimental Brain Research*, *139*, 318–332.
- Mohler, B. J., Thompson, W. B., & Creem-Regehr, S. H. (2006). Absolute egocentric distance judgments are improved after motor and cognitive adaptation within HMD [Abstract]. *Journal of Vision*, *6*(6): 725., <http://journalofvision.org/6/6/725/>, doi:10.1167/6.6.725. [Abstract]
- Multon, F., & Olivier A. H. (2013) Biomechanics of walking in real world: naturalness we wish to reach in virtual reality. In: F. Steinicke, Y. Visell, J. Campos, & A. Lécuyer (Eds.), *Human walking in virtual environments: Perception, technology, and applications* (pp 55–77). New York: Springer.
- Palmisano, S., Allison, R. S., Ash, A., Nakamura, S., & Apthorp, D. (2014). Evidence against an ecological explanation of the jitter advantage for vection. *Frontiers in Psychology*, *5*, 1297.
- Palmisano, S., Allison, R. S., Kim, J., & Bonato, F. (2011). Simulated viewpoint jitter shakes sensory conflict accounts of vection. *Seeing and Perceiving*, *24*, 173–200.
- Palmisano, S., Gillam, B. J., & Blackburn, S. G. (2000). Global-perspective jitter improves vection in central vision. *Perception*, *29*, 57–67.
- Palmisano, S., & Kim, J. (2009). Effects of gaze on vection from jittering, oscillating, and purely radial optic flow. *Attention, Perception, & Psychophysics*, *71*, 1842–1853.
- Palmisano, S., Kim, J., & Freeman, T. C. A. (2012). Horizontal fixation point oscillation and simulated viewpoint oscillation both increase vection in depth. *Journal of Vision*, *12*(12):15, 1–14, <http://www.journalofvision.org/content/12/12/15>, doi:10.1167/12.12.15. [PubMed] [Article]
- Plumert, J. M., Kearney, J. K., Cremer, J. F., & Recker, K. (2005). Distance perception in real and virtual environments. *ACM Transactions on Applied Perception (TAP)*, *2*, 216–233.
- Piryankova, I. V., De La Rosa, S., Kloos, U., Bühlhoff, H. H., & Mohler, B. J. (2013). Egocentric distance perception in large screen immersive displays. *Displays*, *34*, 153–164.
- Redlick, F. P., Jenkin, M., & Harris, L. R. (2001). Humans can use optic flow to estimate distance of travel. *Vision Research*, *41*, 213–219.
- Sekiya, N., & Nagasaki, H. (1998). Reproducibility of the walking patterns of normal young adults: Test-

- retest reliability of the walk ratio (step-length/step-rate). *Gait & Posture*, 7, 225–227.
- Seno, T., Palmisano, S., & Ito, H. (2011). Independent modulation of motion and vection aftereffects revealed by using coherent oscillation and random jitter in optic flow. *Vision Research*, 51, 2499–2508.
- Schmidt, F., & Tiffin, J. (1969). Distortion of drivers' estimates of automobile speed as a function of speed adaptation. *Journal of Applied Psychology*, 53, 536.
- Srinivasan, M. V., Zhang, S., Altwein, M., & Tautz, J. (2000). Honeybee navigation: Nature and calibration of the "odometer." *Science*, 287, 851–853.
- Terziman, L., Lécuyer, A., Hillaire, S., & Wiener, J. M. (2009). Can camera motions improve the perception of traveled distance in virtual environments? [Abstract]. *Proceedings of IEEE Virtual Reality, 2009. VR 2009. IEEE*, (pp. 131–134).
- Terziman, L., Marchal, M., Multon, F., Arnaldi, B., & Lécuyer, A. (2013). Personified and multistate camera motions for first-person navigation in desktop virtual reality. *IEEE Transactions on Visualization and Computer Graphics*, 19, 652–661.
- Thompson, W. B., Gooch, A. A., Willemsen, P., Creem-Regehr, S. H., Loomis, J. M., & Beall, A. C. (2003). Compression of distance judgments when viewing virtual environments using a head mounted display [Abstract]. *Journal of Vision*, 3(9): 18,, <http://journalofvision.org/3/9/18>, doi:10.1167/3.9.18. [Abstract]